



Common Pb of UHP metamorphic rocks from the CCSD project (100–5000 m) suggesting decoupling between the slices within subducting continental crust and multiple thin slab exhumation

Shuguang Li^{a,*}, Chenxiang Wang^a, Feng Dong^a, Zhenhui Hou^a, Qiuli Li^b, Yican Liu^a, Fang Huang^c, Fukun Chen^b

^a CAS Key Laboratory of Crust–Mantle Materials and Environments, School of Earth and Space Sciences, University of Science and Technology of China, Hefei 230026, China

^b Institute of Geology and Geophysics, Chinese Academy of Sciences, Beijing 100029, China

^c Department of Geology, University of Illinois at Urbana-Champaign, 245 NHB, 1301 W. Green St., IL 61801, USA

ARTICLE INFO

Article history:

Received 20 December 2007

Received in revised form 17 May 2008

Accepted 11 September 2008

Available online 23 September 2008

Keywords:

Chinese Continental Scientific Drilling (CCSD) project

UHP metamorphic rocks

Common Pb isotopes

Dabie–Sulu

Detachment within continental crust

ABSTRACT

In order to understand the vertical structure of the Dabie–Sulu ultrahigh-pressure metamorphic (UHPM) belt, common Pb isotopic compositions of omphacites in eclogites and feldspars in gneisses from the Chinese Continental Scientific Drilling (CCSD) project (100–5000 m) have been investigated in this study. Samples from 0 to 800 m (unit 1) in the drilling core have moderately high radiogenic Pb isotopes with small variations of $^{206}\text{Pb}/^{204}\text{Pb}$ (16.82–17.38), $^{207}\text{Pb}/^{204}\text{Pb}$ (15.37–15.49), and $^{208}\text{Pb}/^{204}\text{Pb}$ (37.21–37.72), indicating either high μ ($^{238}\text{U}/^{204}\text{Pb}$) or high initial Pb isotope ratios of their protoliths. In contrast, the samples from 1600 to 2040 m (unit 3) and most of samples from 3200 to 5000 m (unit 5) have moderately or very unradiogenic Pb (unit 3: $^{206}\text{Pb}/^{204}\text{Pb}$ from 16.05 to 16.46, $^{207}\text{Pb}/^{204}\text{Pb}$ from 15.22 to 15.29, and $^{208}\text{Pb}/^{204}\text{Pb}$ from 36.68 to 37.48; unit 5: $^{206}\text{Pb}/^{204}\text{Pb}$ from 15.52 to 15.69, $^{207}\text{Pb}/^{204}\text{Pb}$ from 15.15 to 15.27, and $^{208}\text{Pb}/^{204}\text{Pb}$ from 36.48 to 37.20), indicating either low μ or low initial Pb isotope ratios of their protoliths. Pb isotopes of samples from 800 to 1600 m (unit 2) and from 2040 to 3200 m (unit 4) in the drilling core with abundant ductile shear zones are intermediate between those of units 1 and 3 or 5 and display larger variations. Pb isotopes combined with the published oxygen isotope data of the CCSD samples reveal the original positions of the five units before the Triassic continental subduction. Units 1, 3, and 5 as three UHPM rock slabs could be derived from the subducted upper continental crust, upper–middle continental crust and lower–middle continental crust, respectively. The ductile shearing zones in units 2 and 4 could be the interfaces where the detachment and decoupling took place between the upper, upper–middle and lower–middle continental crusts. The detachment between the upper slab and subducting continental lithosphere probably occurred during continental subduction, and the upper slab (unit 1) was uplifted to a shallow depth along the detachment surface by thrusting. Units 3 and 5 may be detached later from the subducted middle and lower crust and uplifted to a shallow level underneath unit 1. The low $\delta^{18}\text{O}$ values (–4.0 to –7.4‰) [Xiao, Y.-L., Zhang, Z.-M., Hoefs, J., Kerkhof, A., 2006. Ultrahigh-pressure Metamorphic Rocks from the Chinese Continental Drilling Project-II Oxygen Isotope and Fluid Inclusion Distributions through Vertical Sections. *Contribution Mineral Petrology* 152, 443–458; Zhang, Z.-M., Xiao, Y.-L., Zhao, X.-D., Shi, C., 2006. Fluid-rock interaction during the continental deep subduction: oxygen isotopic profile of the main hole of the CCSD project. *Acta Petrologica Sinica* 22 (7), 1941–1951.] in units 2 and 4 suggest that the detachment interfaces could be developed along an ancient fault zones which were the channels of meteoric water activity during the Neoproterozoic.

© 2008 Elsevier B.V. All rights reserved.

1. Introduction

The exhumation of ultrahigh-pressure metamorphic (UHPM) rocks from a depth of >100 km is a hot topic in the geological community. Two mechanisms of exhumation of the UHPM rocks have been

proposed. Namely, the bulk subducted continental crust was detached from the underlying lithosphere mantle and then exhumed (e.g., Chemenda et al., 1995; Hacker et al., 2000; Massonne, 2005); or several HP-UHP metamorphic crustal slices are produced by decoupling between the crust slices on different depth levels within subducted continental crust and the multiple UHPM rock slices are successively exhumed (Li et al., 2003a, 2005b; Xu et al., 2006a; Liu et al., 2007).

* Corresponding author. Tel.: +86 551 3607647.
E-mail address: lsg@ustc.edu.cn (S. Li).

The multi-slice exhumation model is mainly based on studies of the Dabie–Sulu UHPM belt in east-central China. The Dabie–Sulu UHPM belt was formed by continental collision between the South China Block and North China Block in the Triassic (e.g. Li et al., 1993, 1994; Rowley et al., 1997; Hacker et al., 1998; Li et al., 2000; Ayers et al., 2002; Liu et al., 2004, 2005a,b; Li et al., 2005a; Liu et al., 2007), which is the largest known UHPM belt on Earth. It is composed of the Dabie UHPM terrane in the west and Sulu UHPM terrane in the east displaced ~500 km to the north by the Tan–Lu fault (Fig. 1) (Li et al., 1993). Both the Dabie and Sulu UHPM terranes can be subdivided into several HP or UHP sub-zones based on their differences in lithology, geochemistry and geochronology, which provides an opportunity to study different exhumation processes for different tectonic units. For the Dabie UHPM terrane, the Northern Dabie zone (NDZ) is different with the Southern Dabie zone (SDZ) in Pb isotopes (Zhang et al., 2001; Li et al., 2003a, 2005b), fluid inclusions (Xiao et al., 2001, 2002),

metamorphic history and ages (Liu et al., 2007), supporting the multi-slice exhumation model. The multi-slice exhumation model for the Sulu UHPM terrane is also supported by the observations of the metamorphism, structure and ages for the different HP and UHP metamorphic zones (Xu et al., 2006a). However, it is not clear whether the individual UHP metamorphic zone on the surface, e.g. the SDZ in the Dabie terrane or the UHP metamorphic zone in the Sulu terrane exhumed as a single slice or multiple slices.

Uranium is a large ion lithophile element, which is more incompatible than Pb in the crustal rock-metamorphic fluid system (Kogiso et al., 1997). The lower continental crust (LCC) is depleted in U due to relatively high-grade metamorphism and thus has relatively low μ ($^{238}\text{U}/^{204}\text{Pb}$) value, while the upper continental crust (UCC) is enriched in U and has high μ value. Therefore, after long time of accumulation of radiogenic daughter isotopes (Pb), the continental crust is characterized as enrichment of radiogenic Pb in the UCC and

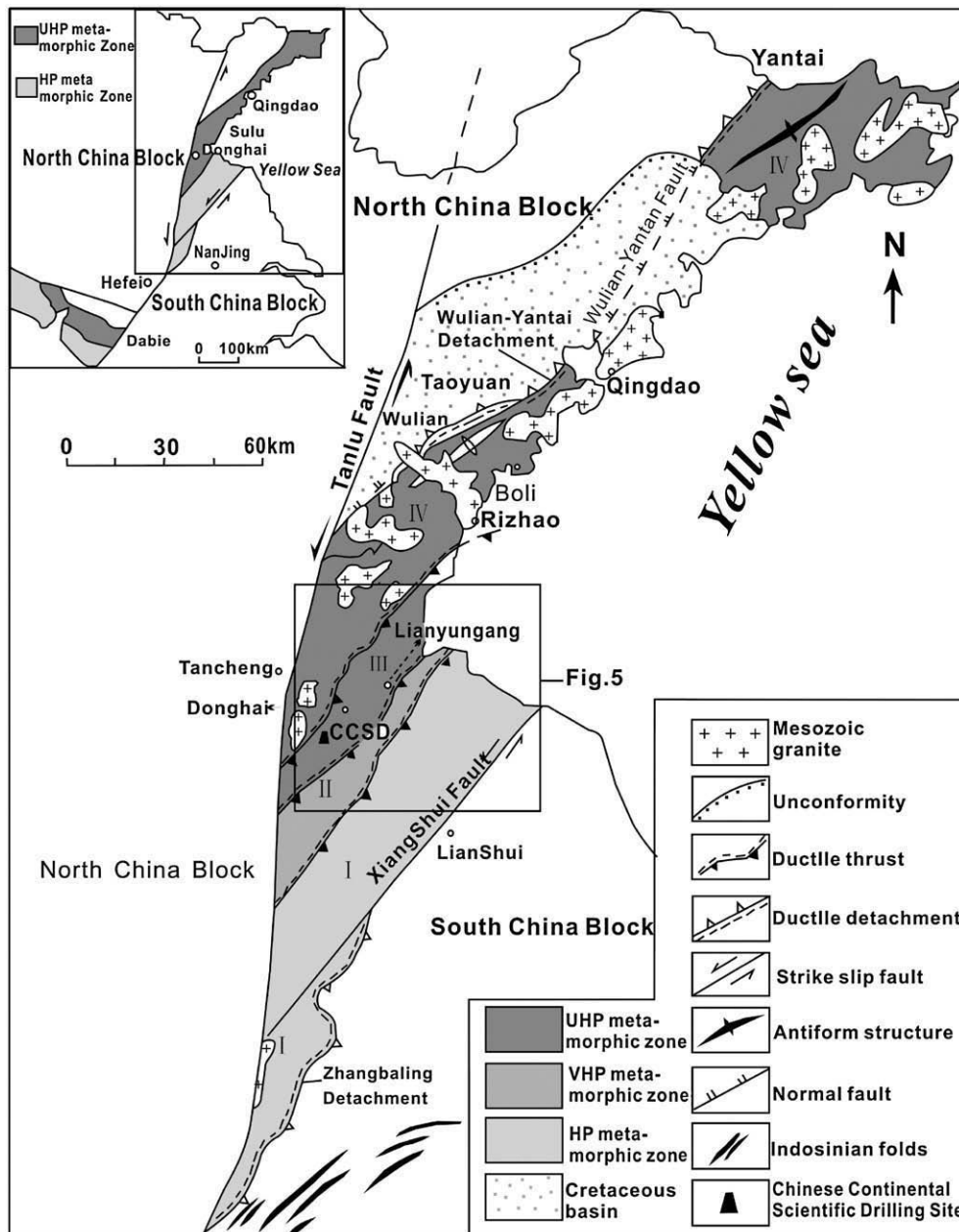


Fig. 1. Tectonic sketch map of the Sulu high-pressure and ultrahigh-pressure (HP-UHP) metamorphic belt, showing: (1) high-pressure zone I, very high-pressure (VHP) zone II, and UHP zones (III and VI) separated by ductile shear zones (modified after Xu et al., 2006a).

unradiogenic Pb in the LCC (Zartman and Doe, 1981). Accordingly, Pb isotopes can be used as a tracer for the original position of rocks in the continental crust. S.-G. Li et al. (2003a) and Zhang et al. (2001) reported the whole-rock U–Pb isotopic compositions for samples from the Dabie region, showing that the Northern Dabie gneisses have the LCC-like Pb isotopes while the Southern Dabie gneisses and eclogites have the UCC-like Pb isotopes. Given the differences in Pb isotopes and lithology and metamorphic history between the NDZ and SDZ, S.-G. Li et al. (2003a, 2005b) and Liu et al. (2007) proposed that the subducted UCC was decoupled from the LCC during the continental subduction along a major thrust fault, by which the deeply subducted UCC was uplifted. Although Pb isotopes are useful means to distinguish nature of crust slices, they have not yet been investigated on the Su–Lu UHPM terrane.

Samples of previous studies on whole-rock U–Pb isotopic compositions were collected on the earth's surface (Zhang et al., 2001; Li

et al., 2003a). However, because the surface samples might have experienced significant weathering and thus U/Pb fractionation, it is questionable whether the whole-rock U/Pb represents the U/Pb of the initial rocks without weathering. The measured U/Pb may not be thus suitable for accurate calculation of the initial Pb isotopic compositions of the whole-rock samples. In order to avoid this problem, one can determine the common Pb isotopes of low U/Pb minerals, which reflect the initial Pb isotopic compositions of the whole rock. Furthermore, previous studies mainly focused on surface samples that cannot provide information on the vertical spatial variation of the UHPM rocks. The Chinese Continental Scientific Drilling (CCSD) project provided an excellent opportunity to continuously sample the UHPM rocks from sub-surface. Here, we report common Pb isotopic compositions of omphacites and feldspars in eclogites and gneisses from the CCSD project. The aims of this paper are: (1) to study the vertical structure of the UHPM zone, (2) to test the decoupling

Table 1

Common Pb isotope compositions of omphacites from eclogite and feldspars from gneiss of the CCSD.

Sample	Lithology	Mineral	Depth (m)	$^{206}\text{Pb}/^{204}\text{Pb}$	$^{207}\text{Pb}/^{204}\text{Pb}$	$^{208}\text{Pb}/^{204}\text{Pb}$	$^{208}\text{Pb}/^{206}\text{Pb}$
*B4R7P2g	Eclogite	Omphacite	108.7	17.211	15.428	37.488	2.178
B79R74P1e	Eclogite	Omphacite	235.18	16.979	15.392	37.403	2.203
*B134R166P1b	Eclogite	Omphacite	323.35	17.233	15.451	37.65	2.185
B149R127P7	Eclogite	Omphacite	347.42	17.327	15.418	37.702	2.176
B154R132P1d	Eclogite	Omphacite	354.90	17.184	15.399	37.563	2.186
*B199R176P6i	Eclogite	Omphacite	433	17.295	15.438	37.65	2.177
B200R177P1l	Eclogite	Omphacite	434.85	17.300	15.407	37.717	2.180
B211R187P2b	Eclogite	Omphacite	452.90	17.343	15.428	37.651	2.171
B218R192P1f	Eclogite	Omphacite	464.65	17.299	15.420	37.602	2.174
B247R210P2u	Eclogite	Omphacite	507.15	17.353	15.420	37.692	2.170
B250R212P1Ca	Eclogite	Omphacite	511.20	17.248	15.396	37.595	2.180
*B261R222P1a	Eclogite	Omphacite	531.50	17.259	15.448	37.663	2.182
B267R224P1f	Eclogite	Omphacite	540.00	17.378	15.486	37.561	2.161
B269R225P4m	Eclogite	Omphacite	543.55	17.363	15.472	37.556	2.163
*B287R235P1a	Eclogite	Omphacite	572.15	16.815	15.372	37.208	2.213
B355R284P1a	Eclogite	Omphacite	687.70	17.155	15.412	37.489	2.185
*B380R298P3s	Eclogite	Omphacite	728.00	17.121	15.415	37.476	2.188
*B552R399P1l	Eclogite	Omphacite	1003.40	16.274	15.369	36.730	2.257
*B578R417P2a	Paragneiss	Plagioclase	1050.25	16.726	15.377	37.28	2.229
*B593R426P1aL	Eclogite	Omphacite	1074.25	16.603	15.355	37.075	2.233
*B655R462P1C	Paragneiss	Orthoclase	1183.40	16.265	15.274	37.091	2.280
*B695R483P6f	Paragneiss	Plagioclase	1262.08	16.670	15.323	37.395	2.243
*B837R572P4C	Orthogneiss	Plagioclase	1615.40	16.362	15.223	37.368	2.284
*B901R599P9b	Paragneiss	K-feldspar	1731.65	16.467	15.253	37.484	2.276
*B926R613P12n	Eclogite	Omphacite	1777.70	16.227	15.273	36.92	2.275
*B992R636P34r	Eclogite	Omphacite	1901.06	16.051	15.223	36.682	2.285
*B1018R64P33a	Eclogite	Omphacite	1939.95	16.293	15.288	37.010	2.272
*B1033R645P6a	Eclogite	Omphacite	1964.36	16.122	15.241	36.828	2.284
*B1046R647P58c	Eclogite	Omphacite	1985.97	16.132	15.237	36.780	2.280
B1100R35P19c	Orthogneiss	K-feldspar	2115.97	16.040	15.287	37.110	2.314
B1209R82P2	Orthogneiss	K-feldspar	2411.44	16.399	15.344	37.433	2.283
B1320R113P77m	Orthogneiss	K-feldspar	2641.62	16.537	15.296	37.718	2.281
B1502R151P21a	Paragneiss	K-feldspar	2958.75	16.521	15.337	37.189	2.251
B1579R14P19h	Orthogneiss	K-feldspar	3093.33	16.201	15.210	37.156	2.293
B1631R33P54u	Orthogneiss	K-feldspar	3260.12	15.812	15.165	36.588	2.314
B1692R49P7g	Orthogneiss	K-feldspar	3391.96	15.960	15.272	37.162	2.329
B1742R61P10a	Orthogneiss	K-feldspar	3481.96	16.210	15.232	37.526	2.315
B1803R79P1d	Orthogneiss	K-feldspar	3610.92	15.803	15.218	37.058	2.345
B1887R15P4c	Orthogneiss	K-feldspar	3730.64	15.519	15.149	36.484	2.351
R1936R30P1d	Orthogneiss	K-feldspar	3830.08	15.644	15.218	36.812	2.353
R1975R41P35d	Orthogneiss	K-feldspar	3901.21	15.768	15.195	36.908	2.341
B2031R53P30r	Orthogneiss	K-feldspar	4001.83	15.777	15.248	37.042	2.348
B2084R65P12d	Orthogneiss	K-feldspar	4100.46	15.722	15.242	37.026	2.355
B2130R75P4d	Paragneiss	K-feldspar	4176.23	15.629	15.170	36.543	2.338
B2169R85P13a	Paragneiss	K-feldspar	4251.51	15.836	15.234	36.912	2.331
B2278R108P1bA	Orthogneiss	K-feldspar	4447.06	16.049	15.209	37.687	2.348
B2291R111P13a	Orthogneiss	K-feldspar	4475.29	16.189	15.207	37.764	2.333
B2388R132P1cA	Orthogneiss	K-feldspar	4644.03	15.847	15.224	37.042	2.337
B2438R142P1uA	Orthogneiss	K-feldspar	4730.31	15.886	15.237	37.119	2.337
B2477R148P23a	Orthogneiss	K-feldspar	4782.41	15.804	15.222	37.039	2.344
B2506R154P41l	Orthogneiss	K-feldspar	4839.96	15.777	15.221	37.009	2.346
B2543R162P1h	Orthogneiss	K-feldspar	4898.99	15.924	15.262	37.204	2.336
B2608R179P21	Orthogneiss	K-feldspar	5028.36	15.73808	15.235	37.033	2.353

*The data are from Dong et al. (2007).

hypotheses within subducting continental crust, and (3) to provide new constraints on the mechanisms of the continental crust subduction and exhumation of the UHPM rocks.

2. Samples and geologic background

The Sulu UHP terrane has been subdivided into 4 sub-zones from south to north, namely, the southern high-pressure zone (I), the central very high-pressure zone (II), and the northern ultrahigh-pressure (UHP) zone (III and IV) (Fig. 1) (Xu et al., 2006a). The drill site of the CCSD project is located in the UHP zone III of the southern segment of the Sulu UHP terrane, near Maobei village (N34°25', E118°40'), about 17 km southwest of Donghai county, Jiangsu Province (Fig. 1). In this region, the Qinglongshan eclogites are well known for the first observation of significantly excess argon (Li et al., 1994) and extremely low $\delta^{18}\text{O}$ (Yui et al., 1995; Zheng et al., 1996; Rumble and Yui, 1998). The main drilling hole of the CCSD project has reached 5148 m in depth. Fifty-four samples were collected from the main drilling hole (100–5000 m in depth) of the CCSD project, which is located above the Maobei eclogite complex in the southwestern of the Maobei shearing tectonic unit. Sample names and depths are listed in Table 1.

The drilling core is mainly composed of eclogites and gneisses. The overall thickness of eclogite is ~1200 m (Fig. 2). Raman spectroscopy shows that coesite inclusions occur in zircons from all types of rocks in the drilling core except the ultramafic rocks (Liu et al., 2001, 2004).

This indicates that most rocks in this drilling core experienced UHP metamorphism. According to the proportion of minor minerals, the eclogites can be divided into quartz eclogite (i.e. high Si eclogite), rutile eclogite (i.e. high Ti and high Ti-Fe eclogite), phengite eclogite (i.e. high Al eclogite), and common eclogite (i.e. high-Mg eclogite and normal eclogite). All eclogites have experienced variable extent of retrograde metamorphism (Zhang et al., 2004). Granitic gneiss or paragneiss is the other rock type in the main drilling hole of the CCSD project from 100 to 5000 m. Most of them are distributed between the range of 1113.14 m to 1596.22 m and below 2050 m (Fig. 2), and others are inter-layered with eclogite layers.

Division of the tectonic and petrologic units in the 100–5000 m drilling core from the CCSD main hole has been studied by numerous authors (e.g., Xu et al., 2004; You et al., 2004; Xu et al., 2006b). Based on lithology, structure and Pb isotopic compositions presented in this paper, we divide the 100–5000 m drilling core into five petrologic units: (1) Unit 1 above 800 m is composed of rutile eclogites with a few layers of ultramafic rocks, gneisses, and amphibolites; (2) Unit 2 from 800 to 1600 m in the drilling core is mainly composed of paragneiss and granitic gneiss with minor ultramafic rocks and eclogites. A series of ductile shearing zone are developed in the depth of 738–1113 m, where mylonitic gneiss and mylonite occur as layers (Chen et al., 2004; Xu et al., 2004). Geophysical studies reveal a strong reflection interface at 1600 m (You et al., 2004), which is a boundary between the overlying mylonitic gneiss and underlying phengite eclogite layer (Zhang et al., 2004); (3) Unit 3 from 1600 m to

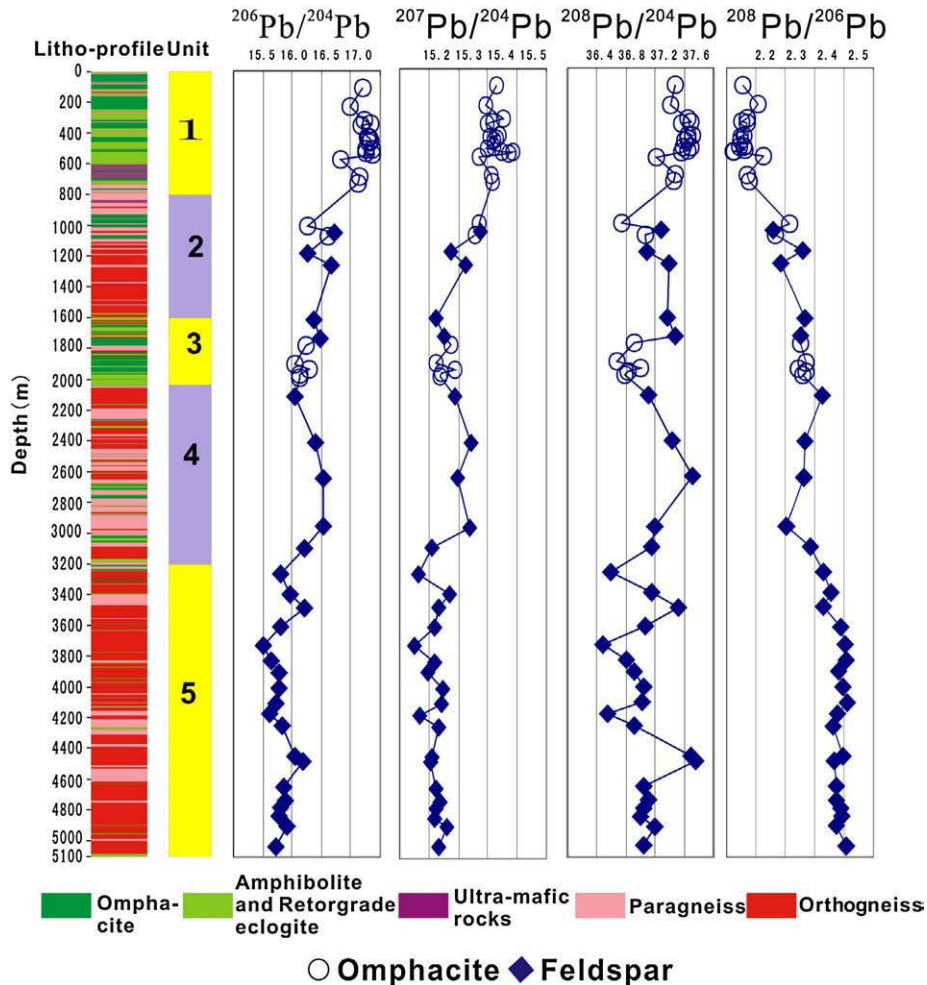


Fig. 2. Common Pb profiles of omphacite from eclogite and feldspar from gneiss of the CCSD project. The lithological profile is modified after Zhang et al. (2004).

2040 m in the drilling core is mainly composed of phengite eclogite with retrograde rutile eclogite and gneiss (Xu et al., 2006b); (4) Unit 4 from 2040 m to 3200 m in the drilling core is mainly composed of paragneiss and granitic gneiss with minor eclogites. Mylonite and mylonitic gneiss occur as layers in the depth of 2650–3090 m suggesting a ductile shearing zone (Xu et al., 2006b); and (5) Unit 5 from 3200 m to 5000 m in the drilling core is mainly composed of granitic gneiss with minor eclogites (Xu et al., 2006b). All these rock units and their intervening shear zones have SE-dipping foliation and SE-plunging stretching lineation (Xu et al., 2006b). However, slight differences in striking and dipping directions between the petrologic units have been recognized. For example, systematic determination of tectonic foliations and lineations indicate different strike-dips between units 1 and 3. Rocks above 1600 m have a lineation striking of ESE (100°E) and dipping of 30–40°, while rocks below 1600 m have a lineation striking SSE (160°E) and dipping over 50° (You et al., 2004). This indicates that units 1 and 3 are not coherent and belong to different UHPM rock slices.

3. Analytical methods

About 2 g of feldspar (plagioclase or K-feldspar) and omphacite were extracted and selected from gneisses and eclogites, respectively, at the Institution of Regional Geology and Mineral Investigation of Hebei. Alteration-free feldspar (40 mg) and omphacite (50–100 mg) handpicked under a binocular microscope were used for Pb isotope analysis.

Pb isotope data were obtained at the Laboratory for Radiogenic Isotope Geochemistry of Institute of Geology and Geophysics, Chinese Academy of Science, using a Finnigan MAT-262 mass spectrometer. Pb was purified by conventional anion-exchange method (AG1-X8, 200–400 resin). About 50 mg mineral separates were rinsed in purified water and HCl for a few times, and then dissolved in a 7 ml Teflon beaker using purified HNO₃ and HF. Pb was extracted by HBr, which was centrifuged for chemical separation and purification. After cleaning the AG1-X8 column using HCl and water, HBr was used to condition the column. Pb was eluted by HBr and finally collected by HCl. A second purification of Pb was conducted before it was measured by mass spectrometry.

The whole procedure blank for Pb is 0.05–0.1 ng. Fractionation of Pb isotopes during mass spectrometer analysis was calibrated against standard NBS981, which give $^{206}\text{Pb}/^{204}\text{Pb} = 16.9376 \pm 0.0015$ (2σ), $^{207}\text{Pb}/^{204}\text{Pb} = 15.4939 \pm 0.0014$ (2σ), and $^{208}\text{Pb}/^{204}\text{Pb} = 36.7219 \pm 0.0033$ (2σ) during the course of this study. The precision for Pb isotope data on the mass spectrometer is better than 0.1%.

4. Pb isotope results

Pb isotopic compositions of 54 samples (feldspars from gneisses and omphacite from eclogites) are listed in Table 1, in which 18 samples from the drilling core (100–2000 m) were analyzed earlier and published as preliminary results in a Chinese journal (Dong et al., 2007) whereas other 36 samples were analyzed in this study to obtain a complete Pb isotopic variation profile for the whole drilling core from 100 to 5000 m. Because Pb isotope data are obtained for two mineral species, two questions have to be asked before discussing their variations.

4.1. Do omphacites from eclogites have low U/Pb?

Feldspar has been widely used to study the common Pb of igneous or metamorphic rocks because of its low U/Pb ratio (e.g., Zhang, 1995). Recent studies show that omphacite from eclogite is also a mineral with low U/Pb. Experiment of partial melting of eclogite shows the greater partition coefficient of Pb than U between clinopyroxene and melt (Klemme et al., 2002). Q.-L. Li et al. (2003b) observed the

consistency between the U–Pb mineral (rutile + omphacite) isochron age and conventional rutile U–Pb concordia age obtained by common Pb correction based on the Pb isotopic composition of omphacite in the same eclogite sample. This suggests that omphacite with low U/Pb ratio ($\mu = 2.8$) can be used for common Pb correction in U–Pb dating of rutile. Therefore, omphacite can be directly used for the study of common Pb, representing the initial Pb isotopes of the whole rock. In this study, we use both feldspar and omphacite to study the initial Pb isotopic ratios and no age correction was performed.

4.2. Are the geochemical implications of the Pb isotopes of feldspar and omphacite comparable?

The feldspar and omphacite mineral separates are derived from gneiss and eclogite, respectively. The protoliths of the eclogites and gneisses from the Dabie–Sulu UHPM zones are the Neoproterozoic mafic and intermediate-felsic rocks, respectively (Zheng et al., 2003; Zhang et al., 2004; Zhao et al., 2005). Although crustal contribution of the latter is greater than the former, the whole-rock Pb isotopic compositions of the eclogites and gneisses from the southern Dabie zone are not different (Zhang et al., 2001; Li et al., 2003a). Results of this study also indicate that feldspars and omphacites from drilling core samples from 800 to 2000 m show similar trend in $^{206}\text{Pb}/^{204}\text{Pb}$ and $^{207}\text{Pb}/^{204}\text{Pb}$ variations (Fig. 2). For instance, there are large amount of gneisses in unit 2 (800–1600 m) drilling core, but two eclogites (B552R399P11 and B593R426P1aL) from the same portion of the drilling core have Pb isotopic compositions consistent with those of the gneisses, both of which show decreasing Pb isotopic ratios with increasing depth. Moreover, comparison of gneisses from unit 3 (1600–2040 m) portion (B837R572P4C and B901R599P9b) with inter-layered eclogites also shows generally similar U–Pb isotopic compositions except for different $^{208}\text{Pb}/^{204}\text{Pb}$ ratios. Notably, feldspars from 1600–2040 m drilling core have higher $^{208}\text{Pb}/^{204}\text{Pb}$ than omphacite (Fig. 1), which could be due to the protolith of the gneisses having greater contribution of the LCC. Therefore, we combine the common Pb of feldspars and omphacites to show Pb isotopic variations with increasing depth and discuss implications of the difference in Pb isotopic compositions between the three units (1, 3, and 5) of the drilling core.

The decreasing of $^{206}\text{Pb}/^{204}\text{Pb}$ and $^{207}\text{Pb}/^{204}\text{Pb}$ ratios and increasing of $^{208}\text{Pb}/^{206}\text{Pb}$ ratios with increasing of the depth are striking features of the Pb isotopic profiles of the CCSD samples (Fig. 2). As shown in Fig. 2, all samples from unit 1 (100–800 m) are omphacite-bearing, while samples from units 2 and 3 contain both omphacite and feldspar, and minerals from units 4 and 5 are feldspar. Pb isotopic composition of samples from unit 1 (100 to 800 m) shows limited variation with $^{206}\text{Pb}/^{204}\text{Pb}$ ranging from 16.82 to 17.38 with average of 17.23, $^{207}\text{Pb}/^{204}\text{Pb}$ from 15.37 to 15.49 with average of 15.42, and $^{208}\text{Pb}/^{204}\text{Pb}$ from 37.21 to 37.72 with average of 37.57. Overall they all have relatively high radiogenic Pb isotopes. Except for $^{208}\text{Pb}/^{204}\text{Pb}$ ratios, samples from unit 3 (1600 to 2040 m) also have uniform but moderately low radiogenic Pb isotopes with $^{206}\text{Pb}/^{204}\text{Pb}$ ranging from 16.05 to 16.47 with average of 16.24 and $^{207}\text{Pb}/^{204}\text{Pb}$ from 15.22 to 15.29 with average of 15.25. As mentioned above, two feldspars from 1600–2040 m drilling core have significantly higher $^{208}\text{Pb}/^{204}\text{Pb}$ than omphacites, and omphacite samples from unit 3 also show uniform low $^{208}\text{Pb}/^{204}\text{Pb}$ from 36.68 to 37.01 with average of 36.86. Except for three samples (B1742R61P10a, B2278R108P1bA, and B2291R111P13a), the other sixteen feldspar separates from unit 5 show uniform and very unradiogenic Pb isotopes with $^{206}\text{Pb}/^{204}\text{Pb}$ ranging from 15.52 to 15.96 (average: 15.78), $^{207}\text{Pb}/^{204}\text{Pb}$ from 15.15 to 15.27 (average: 15.22) and $^{208}\text{Pb}/^{204}\text{Pb}$ from 36.48 to 37.20 (average: 36.94). Although the $^{208}\text{Pb}/^{204}\text{Pb}$ ratios of unit 5 show a large variation ranging from 36.48 to 37.76, they have uniform and high $^{208}\text{Pb}/^{206}\text{Pb}$ ratios from 2.42 to 2.50, reflecting the uniform and high Th/U ratios in protolith of unit 5. In contrast, unit 1 and unit 2 have low and moderately low

$^{208}\text{Pb}/^{206}\text{Pb}$ ratios, respectively, reflecting their relative lower Th/U ratios in their protoliths. The different Pb isotopic compositions of units 1, 3, and 5 clearly indicate that they were from different depths in the subducted continental crust.

Moreover, the Pb isotopic compositions of samples from unit 2 (800–1600 m) and unit 4 (2040–3200 m) of the drilling core also show transitional trends between units 1 and 3 and between units 1 and 5, respectively (Fig. 2). For unit 2, the $^{206}\text{Pb}/^{204}\text{Pb}$ varies from 16.27 to 16.73 (average: 16.51), $^{207}\text{Pb}/^{204}\text{Pb}$ from 15.27 to 15.38 (average: 15.34), and $^{208}\text{Pb}/^{204}\text{Pb}$ from 36.73 to 37.40 (average: 37.11), which are in between units 1 and 3. While for unit 4, the $^{206}\text{Pb}/^{204}\text{Pb}$ varies from 16.04 to 16.54 (average: 16.34), $^{207}\text{Pb}/^{204}\text{Pb}$ from 15.21 to 15.34 (average: 15.29), and $^{208}\text{Pb}/^{204}\text{Pb}$ from 37.11 to 37.72 (average: 37.32), which are higher than those of unit 3 and in between units 1 and 5.

5. Discussion

5.1. Pb isotopic constraints on original positions of the UHP units in the subducted continental crust

In the $^{207}\text{Pb}/^{204}\text{Pb}_i$ vs. $^{206}\text{Pb}/^{204}\text{Pb}_i$ diagram (Fig. 3A), the drilling core samples from units 1 and 5 clearly have different Pb isotope compositions with unit 1 samples having moderately high radiogenic Pb and unit 5 samples having unradiogenic Pb. Samples from units 2, 3, and 4 have intermediate $^{207}\text{Pb}/^{204}\text{Pb}$ and $^{206}\text{Pb}/^{204}\text{Pb}$ ratios. While $^{206}\text{Pb}/^{204}\text{Pb}$ and $^{207}\text{Pb}/^{204}\text{Pb}$ ratios of the drilling core samples of this study are significantly lower than the values of UHP paragneiss and eclogite nodule in marble from the Dabie orogen (Zhang et al., 2001; Li et al., 2003a) as well as the MORB and EMII (Zindler and Hart, 1986), they are generally similar to the values of eclogites and UHP orthogneiss (Zhang et al., 2001; Li et al., 2003a) as well as the post-collisional mafic–ultramafic intrusive (PCMI) rocks (Wang et al., 2005; Huang et al., 2007) from the Dabie orogen (Fig. 3A). Radiogenic Pb isotopes of the samples from unit 1 are in good agreement with omphacites from the Dabie eclogites (Fig. 3A) which were considered to be derived from subducted upper continental crust (Li et al., 2003a; Liu et al., 2007). In contrast, the samples from unit 5 have unradiogenic Pb isotopes and most of them are obviously lower than the values of the post-collisional mafic–ultramafic intrusive rocks from the Dabie orogen from a mantle source intensely affected by the recycled deeply subducted mafic lower crust from the South China Block (Huang et al., 2007), and close to the ancient “lower mafic continental crust” in the Dabie orogen (Huang et al., 2008) (Fig. 3A).

In addition, samples from the CCSD project (100–5000 m) show three trends in the $^{208}\text{Pb}/^{204}\text{Pb}$ vs. $^{206}\text{Pb}/^{204}\text{Pb}$ figure (Fig. 3B). Samples from unit 5 are arranged in left trend showing higher $^{208}\text{Pb}/^{204}\text{Pb}$ than other unit samples given a similar $^{206}\text{Pb}/^{204}\text{Pb}$; samples from units 2, 3 and 4 are in middle trend, in good agreement with the post-collisional mafic–ultramafic intrusive rocks from the Dabie orogen; and samples from unit 1 are arranged in right trend with relative lower $^{208}\text{Pb}/^{204}\text{Pb}$ ratios falling out of the area of the post-collisional mafic–ultramafic intrusive rocks from the Dabie orogen, but overlapping eclogite samples from the SDZ in the Dabie orogen (Fig. 3B). The difference in $^{208}\text{Pb}/^{204}\text{Pb}$ ratios between the rock units of the CCSD project (100–5000 m) suggests that the protolith from unit 5 is characterized by low μ and high Th/U, which is a typical feature of the lower continental crust (LCC), while the protolith of samples from unit 1 is characterized by high μ and low Th/U, a typical feature of the upper continental crust (UCC) (Zartman and Doe, 1981). The consistence in Pb isotopes between unit 1 of the CCSD drilling core and the eclogites from the SDZ also suggests that unit 1 is derived from the subducted upper continental crust, because the SDZ in the Dabie eclogites are considered to be derived from subducted upper continental crust (Li et al., 2003a; Liu et al., 2007).

The above discussions are based on the assumption that the protolith of the eclogites and granitic gneisses from the CCSD drilling

core had similar initial Pb isotopic compositions. If so, the observed systematic difference in Pb isotopes should be due to the difference in the μ values and Th/U ratios of the protoliths and reflect their different depth before continental subduction. The radiogenic Pb isotopes of samples from unit 1 may reflect the high μ and low Th/U of the protolith in the UCC, while the unradiogenic Pb isotopes of samples from unit 5 may reflect the low μ and high Th/U of the protolith that originated from the LCC. However, the Pb isotopic compositions of the UHPM rocks depend on both initial Pb isotopic compositions and μ value of the protolith. If the protolith of the samples from unit 5 originally had low $^{206}\text{Pb}/^{204}\text{Pb}$ and high $^{208}\text{Pb}/^{204}\text{Pb}$, the observed difference in Pb isotopic compositions between units could be due to the Pb isotopic heterogeneity in their protoliths with similar μ values. Therefore, we need to consider oxygen isotope geochemistry to give

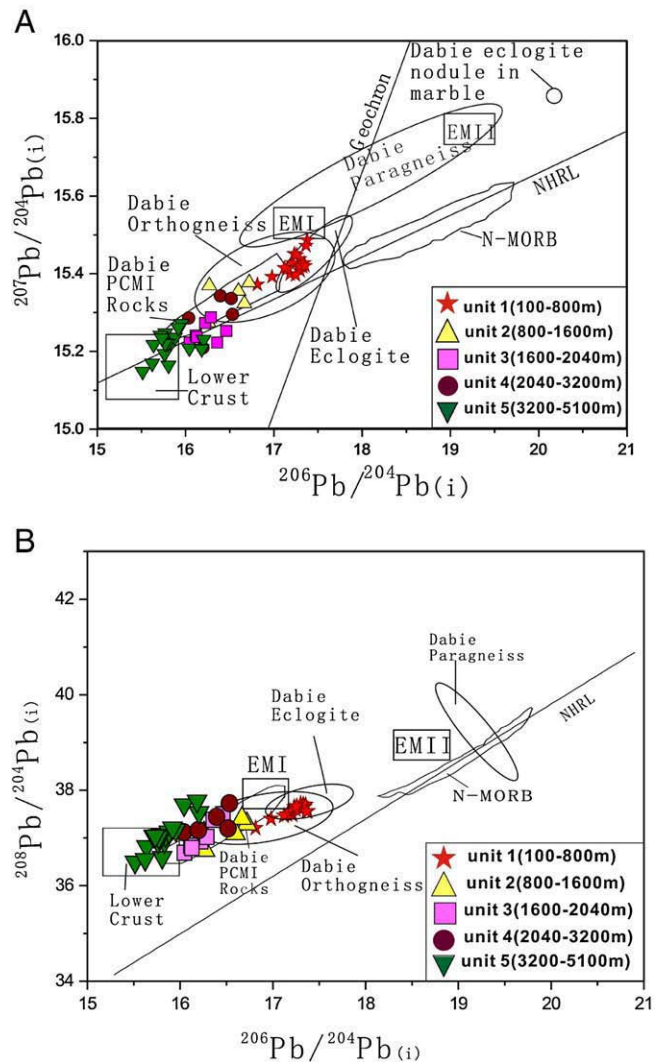


Fig. 3. $^{207}\text{Pb}/^{204}\text{Pb}$ – $^{206}\text{Pb}/^{204}\text{Pb}$ and $^{208}\text{Pb}/^{204}\text{Pb}$ – $^{206}\text{Pb}/^{204}\text{Pb}$ diagrams showing the comparison between common Pb of omphacite from eclogite and feldspar from gneiss of the CCSD project and initial Pb isotopic compositions ($t = 230$ Ma) of the rocks from the Dabie orogen. Data source: lower continental crust (LCC) are from the unradiogenic Pb endmember of the Mesozoic granites and high-Mg adakites from the Dabie orogen (Huang et al., 2008); N-MORB, EMI and EMII are from Zindler and Hart (1986); the post-collisional mafic–ultramafic intrusive (PCMI) rocks from Dabie orogen are from Huang et al. (2007) and Wang et al. (2005); eclogite, orthogneiss, paragneiss and eclogite nodule in marble from the Dabie orogen are from Zhang et al. (2001), S.-G. Li et al. (2003a) and Li et al. (unpublished data). Because of lack of Th data for some whole-rock samples, the fields of paragneiss and eclogite nodule in marble from the Dabie orogen in $^{208}\text{Pb}/^{204}\text{Pb}$ – $^{206}\text{Pb}/^{204}\text{Pb}$ diagram are smaller than that in $^{207}\text{Pb}/^{204}\text{Pb}$ – $^{206}\text{Pb}/^{204}\text{Pb}$ diagram or absent, respectively.

more constraints on the reasons for the isotopic difference between the upper and lower units of the drilling core.

5.2. Oxygen isotope constraints on original positions of the UHP units in subducted continental crust

Oxygen isotopic study indicates that samples from unit 1 (0–800 m) generally have low $\delta^{18}\text{O}$ (Xiao et al., 2006) (Fig. 4), suggesting that the protolith should be at shallow crustal level in the Neoproterozoic and interacted with meteoric water (Zheng et al., 2003). Samples from unit 2 and unit 4 have very low $\delta^{18}\text{O}$ values with the negative $\delta^{18}\text{O}$ anomaly occurring at 971–1003 m ($\delta^{18}\text{O} = -4.8 \sim -6.5$), 2552–2699 m ($\delta^{18}\text{O} = -7.4 \sim -4.0$), and 3053–3062 m ($\delta^{18}\text{O} = -1.3 \sim -3.1$), respectively (Fig. 4) (Xiao et al., 2006; Zhang et al., 2006). Such low $\delta^{18}\text{O}$ values indicate strong water–rock interaction in the Neoproterozoic, suggesting that the 971–1003 m, 2552–2699 m, and 3053–3062 m intervals could be meteoric channels related to ancient fault zones. As mentioned above, several ductile shear zones are developed at those intervals with negative $\delta^{18}\text{O}$ anomaly in the drilling core. On the contrary, samples from unit 3 (1600–2040 m) and unit 5 (3200–5000 m) have $\delta^{18}\text{O}$ of typical normal metamorphic rocks ($\geq 5.6\text{‰}$) and omphacites from eclogites having $\delta^{18}\text{O}$ of $\sim 5.6\text{‰}$ within the range of normal mantle peridotite (Fig. 4) (Xiao et al., 2006; Zhang et al., 2006). This indicates that the protoliths of units 3 and 5 could be located at relatively deep level avoiding significant water–rock interaction in the Neoproterozoic. However, the original protolith depth of unit 3 could not be too deep because of the existence of two low $\delta^{18}\text{O}$ zones at 2552–2699 m and 3053–3062 m of the drilling core (Fig. 4) (Xiao et al., 2006; Zhang et al., 2006). The repeating low $\delta^{18}\text{O}$ zones suggest that the meteoric water can enter the middle continental crust (MCC) level through a series of fault “channels”. Previous studies show that meteoric water can enter the top of the MCC through a series of fault zones to react with rocks at depths of 10–15 km (Taylor, 1990). Therefore, the protolith of the samples from unit

3 could be at the upper–middle continental crust above 15 km and the protolith of the samples from unit 5 could be at a deeper level below 15 km because no low $\delta^{18}\text{O}$ zone has been observed below 3200 m in the drilling core. In summary, oxygen isotopic data suggests that the protoliths of the samples from units 1, 3, and 5 were originally at the UCC, upper-MCC and lower-MCC depths, respectively. Accordingly, the samples from unit 5 should have the lowest μ values, unit 1 has the highest μ values, and unit 3 has the intermediate. This is consistent with the implication from their Pb isotope compositions, i.e. the samples from the lower unit are more enriched in unradiogenic Pb isotopes than the samples from the upper unit (Fig. 3).

Based on the U–Pb isotopic composition of whole rocks from the Dabie orogen, S.-G. Li et al. (2003a) proposed that detachment and decoupling could occur between the UCC and LCC, and the detached upper subducted crust slice was exhumed firstly by thrust along the detached interface. In this study, we conclude that the rock units 1, 3 and 5 of the drilling core in the Sulu UHPM Zone (III) (Xu et al., 2006a) are derived from the UCC, upper-MCC and lower-MCC, respectively. This not only reinforces the suggestion by S.-G. Li et al. (2003a) but also proves the multi-slab decoupling during exhumation including decoupling between the subducted UCC and MCC as well as between the upper-MCC and the underlying lower-MCC.

5.3. The detachment and decoupling interfaces between the UHPM crust slices

The ductile shearing zones in units 2 and 4 of the drilling core from the CCSD project could be the interfaces where the detachment and decoupling between the UCC, upper-MCC and lower-MCC happened. Considering that the 738–1113 m ductile shear zone is characterized by deformation of eclogitic phases (Chen et al., 2004), such detachment within the subducted continental crust could happen during the subduction process. This study shows that the detachment interface occurring within the continental crust was a fault zone as a channel of meteoric water activity in the Neoproterozoic. The strong water–rock interaction resulted in the enrichment of H_2O in the fault zone and adjacent rocks and consequently a zone with low viscosity, which is critical for the later inner-crustal detachment and decoupling between the UCC, MCC, and LCC. Experiment models show that the UCC can be uplifted during subduction along the detachment surface (Chemenda et al., 1995). Modeling results of lithospheric viscosity–depth curves based on reasonable assumptions of geotherms and lithospheric composition suggest that there are at least two low-viscosity zones within continental crust at different depths (Meissner and Mooney, 1998). This study suggests that the realistic low-viscosity zones could be much more than the modeling results because of the existence of large fault zones in the crust. Accordingly, with increasing the depth of subduction, multiple slices in the subducting continental crust could be decoupled along the low-viscosity zones creating multi detachment surfaces within the continental crust (Meissner and Mooney, 1998).

As shown in Figs. 2 and 3, Pb isotopes of the samples from unit 2 show a transitional trend from unit 1 to unit 3. The Pb isotopic variations may indicate mixing between units 1 and 3 at the detachment interface and its adjacent area. Such big-scale ($n \times 100$ m) mixing requires the presence of fluids. As mentioned above, the extremely low $\delta^{18}\text{O}$ and enrichment of H_2O -bearing minerals in eclogites and gneisses in unit 2 suggest that it was a main channel for fluid activity in the Neoproterozoic (Xiao et al., 2006; Zhang et al., 2006). However, the detachment interface in the continental crust could be also the main channel during the subduction of the continental crust. Therefore, based on the Pb isotopic data of unit 2 only, it is not clear when the Pb isotopic mixing occurred in unit 2.

Figs. 2 and 3 also show that Pb isotopic ratios of the samples from unit 4 are slightly higher than those of unit 3, thus their Pb isotopes show a transitional trend from unit 1 to unit 5 but not from unit 3 to unit 5. This suggests that the Pb isotopic mixing could only occur due to the presence of meteoric water activity through fault zones in the

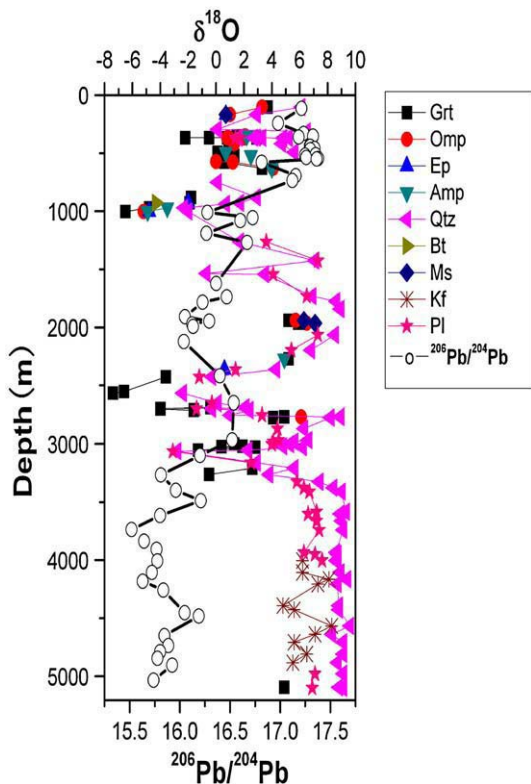


Fig. 4. Comparison between lead and oxygen isotopic compositions of the CCSD core (100–5000 m). Data source: lead isotopic data are from Table 1; oxygen isotopic data are from Zhang et al. (2006).

Neoproterozoic, because movement of meteoric water along channels can carry Pb from the earth's surface to the depth. Metamorphic fluid activity in the detachment interface between the UHPM crust slices during the subduction of the continental crust may only cause the Pb isotopic mixing between the adjacent UHPM crust slices, i.e. the Pb isotopes of unit 4 should be produced by mixing of Pb from units 3 and 5, however, which is not observed.

In summary, the Pb isotopic mixing occurred in units 2 and 4 most probably occurred by meteoric water activity through fault zones in the Neoproterozoic. The metamorphic fluid activity in the detachment interface between the UHPM crust slices during the subduction of the continental crust may not be strong enough to significantly effect on the Pb isotopes of the ductile shearing zones.

5.4. Connection between the rock units in the drilling core and tectonic slices on the surface

Based on surface geology, Xu et al. (2006a) subdivided the UHP zone III into 4 tectonic slices from SE to NW, namely the Lianyungang (IIIa), Maobei (IIIb), Donghai (IIIc), and Shilianghe (IIId) slices, which are separated by ductile shear zones (DF6, DF7, and DF8, respectively) with abundant mylonites and mylonitic rocks (Fig. 5). These tectonic slices and their intervening shear zones have SE-dipping foliations

and SE-plunging stretching lineations (Xu et al., 2006a). Because the main drilling hole (5000 m in depth) of the CCSD project is located above the Maobei tectonic slice (IIIb) (Fig. 5), and according to the three UHPM crust slices (i.e. units 1, 3 and 5) recognized from the drilling core (100–5000 m) in this study, it is reasonable to suggest that the main drilling hole of the CCSD project may pass through the Maobei (IIIb) (unit 1) and Donghai (IIIc) (unit 3) slices, and get into the Shilianghe (IIId) (unit 5) slice. Accordingly, units 2 and 4 with ductile shearing zones may connect to the DF7 and DF8 on the surface, respectively. This study also suggests that the UHP zone III in the SuLu terrane is an assemblage of exhumed UHPM crust slices derived from different crust levels. The interfaces between the UHPM crust slices are ancient fault zones with low viscosity which were main channels for fluid activity during neo-Proterozoic time.

5.5. Comparison between the Dabie and Su–Lu UHPM zones

The Dabie UHPM belt can be subdivided in to 4 HP-UHP metamorphic zones from the south to the north, i.e. (1) Northern Yangtze blueschist zone, (2) Hong'an-Susong cold eclogite zone, (3) Southern Dabie UHPM zone, and (4) Northern Dabie high temperature UHPM zone. It is well accepted that the Southern Dabie UHPM zone and the Su–Lu UHP zone III are comparable in petrology and geochronology, because both of them

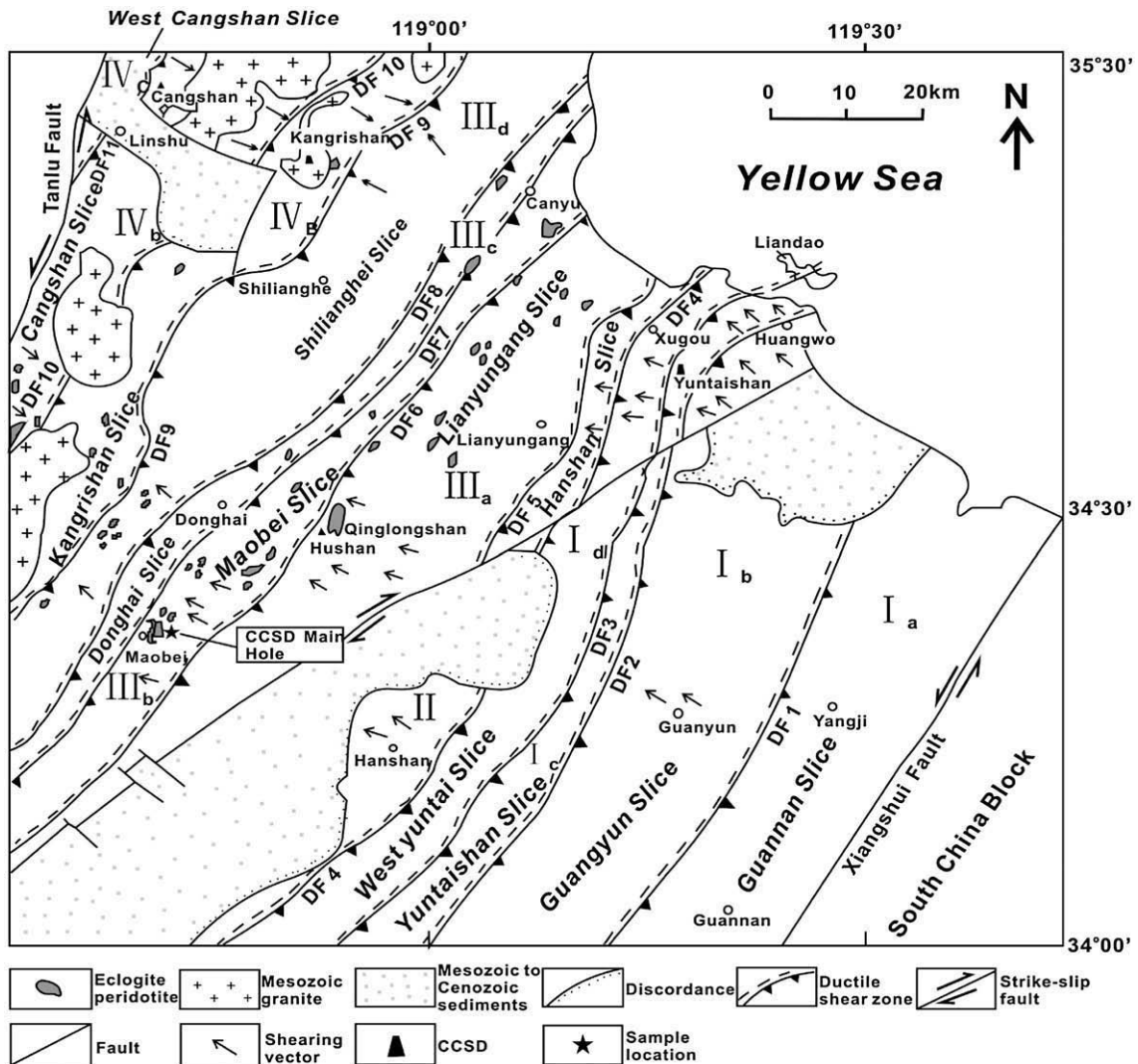


Fig. 5. Tectonic map of the Lianyungang area showing the distribution of various high-pressure and ultrahigh-pressure slices and major ductile shear zones. CCSD – Chinese Continental Scientific Drilling (modified after Xu et al., 2006a).

contain coesite or diamond-bearing eclogite (Xu et al., 1992; Cong et al., 1995; Zhang et al., 1995; Liu et al., 2001) and experienced the peak UHP metamorphism at 226 ± 3 Ma or 227 ± 4 Ma (Li et al., 1994, 2000; Li et al., 2005a; Liu et al., 2005b). The surface rocks in the Southern Dabie UHPM zone are characterized by the UCC features (Zhang et al., 2001; Li et al., 2003a). $^{206}\text{Pb}/^{204}\text{Pb}$ ratios of the UHP paragneiss and eclogite nodule in marble in the Southern Dabie UHPM zone are higher than 18.50 (Fig. 3), but no such high radiogenic Pb isotopes have been observed in the samples from the drilling core of the CCSD. $^{206}\text{Pb}/^{204}\text{Pb}$ ratios of all the samples including paragneiss from the drilling core are lower than 17.40 (Table 1 and Fig. 3). As mentioned above, all rock units in the drilling core of the CCSD project can be connected with the surface UHP sub-zones Maobei (IIIb), Donghai (IIIc), and Shilianghe (IIId) in the Su–Lu UHP zone III. If the UHPM rocks exposed on the surface in the Su–Lu UHP zone III have similar Pb isotopic compositions to the samples from the drilling core, the differences in Pb isotopic compositions of the UHPM rocks between the Southern Dabie UHPM zone and drilling core of the CCSD project suggest that the protoliths of the UHPM rocks in the Su–Lu UHP zone III were originally at a deeper level in the subducted continental crust than the surface rocks in the Southern Dabie UHPM zone. Geophysical study shows that the deep Southern Dabie UHPM zone is composed of a series of thin rock slices (Dong et al., 2004). Among these slices, there are two groups of rock slices with the first one from 7 to 15 km containing several UHPM rock slices and the second one from 15–25 km similar to gneisses in the northern Dabie zone. We envisage that the features of the first group of rocks slice in the deep Southern Dabie UHPM zone (7 to 15 km) may be similar to the rock slices in the Su–Lu UHP zone III. Therefore, both the Su–Lu UHPM zone III and Southern Dabie UHPM zone could be formed via imbricated crust slices from the subducted UCC, upper-MCC and lower-MCC. This study strongly supports the multi-slice exhumation model for the UHPM rocks in continental collision orogen and reveals that even one UHP metamorphic zone on the surface could be formed by multiple crustal slices derived from different depth levels.

6. Conclusions

Based on the study of the Pb isotopes of the omphacites in eclogites and feldspars in gneisses from the CCSD project, two conclusions can be drawn:

(1) The samples from unit 1 (100–800 m), unit 3 (1600–2000 m) and unit 5 (3200–5000 m) in the drilling core of the CCSD project show systematic difference in the Pb isotopes. Samples from unit 1 have moderately high radiogenic Pb, samples from unit 3 have moderately unradiogenic Pb whereas samples from unit 5 have very unradiogenic Pb. Pb isotopes and oxygen isotopes data indicate that units 1, 3 and 5 of the drilling core could be derived from the subducted UCC, upper-MCC and lower-MCC, respectively. The ductile shearing zones in unit 2 (800 to 1600 m) and unit 4 (2040–3200) of the drilling core could be the detachment interface between the UCC, upper-MCC and lower-MCC. The detachment and decoupling happened during continental subduction, so that the upper UHPM rock slice (unit 1) was uplifted to a shallow depth along the detachment interface by thrust. Unit 3 UHPM rock slice may be detached from the subducting middle crust latter and can also be uplifted to a shallow depth below unit 1 slice. The following detachment could occur between the lower-MCC and LCC to produce unit 5 UHPM rock slice, which was uplifted to a shallow place below unit 3. This not only reinforces previous multi-slice exhumation model (Li et al., 2005b; Xu et al., 2006a; Liu et al., 2007), but also suggests that the Su–Lu UHP zone III and Southern Dabie UHPM zone, which have been considered to be a single exhumed UHPM slab previously, could be formed via imbricated crust slices from different depth levels in the subducted continental crust.

(2) Pb isotopic compositions of samples from unit 2 (800 m to 1600 m) and unit 4 (2040–3200 m) show transitional features between units 1 and 3 or 5, respectively, which could be due to

mixing processes between units 1 and 3 or 5 portions due to hydrous fluid activity in the Neoproterozoic. The ductile shear zones may be active along the detachments between units 1 and 3 or 5 UHPM crust slices and were developed on some ancient fault zones. The ancient fault zones were the main channels for meteoric water activity during the Neoproterozoic time, resulting in low-viscosity zones. Thus, the realistic low-viscosity zone numbers could be much larger than the previous modeling results (e.g. Meissner and Mooney, 1998) because of the existence of large fault zones in the crust.

Acknowledgements

This study was financially supported by the State Key Basic Research Developed Program (2003CB716500) and the Natural Science Foundation of China (No. 40634023 and 40773013) as well as Chinese Academy of Science (kzcx2-yw-131). We thank Prof. Xu Zhiqin and all scientists and technicians working on the CCSD project for their help to collect the samples from drilling core. We also thank Prof. Xiao Yilin for a helpful discussion and references providing.

References

- Ayers, J.C., Dunkle, S., Gao, S., Miller, C.F., 2002. Constraints on timing of peak and retrograde metamorphism in the Dabie Shan ultrahigh-pressure metamorphic belt, east-central China, using U–Th–Pb dating of zircon and monazite. *Chemical Geology* 186, 315–331.
- Chemenda, A.I., Mattauer, M., Malavieille, J., Bokun, A.N., 1995. A mechanism for syn-collisional rocks exhumation and associated normal faulting: results from physical modeling. *Earth and Planetary Science Letters* 132, 225–232.
- Chen, Y., Jin, Z.-M., Ou, X.-G., Jin, S.-Y., Xu, H.-J., 2004. Deformation features of gneiss and UHP eclogite from ductile shear zone and its relation with seismic velocity anisotropy: evidences from core samples at 680–1200 m of CCSD. *Acta Petrologica Sinica* 20 (1), 97–108 (in Chinese with English abstract).
- Cong, B.-L., Zhai, M.-G., Carswell, D.A., Wilson, R.N., Wang, Q.-C., Zhao, Z., 1995. Petrogenesis of ultrahigh-pressure rocks and their country rocks at Shuanghe in Dabieshan, Central China. *Eur. J. Mineral.* 7, 119–138.
- Dong, S.-W., Gao, R., Cong, B.-L., Zhao, Z.-Y., Liu, X.-C., Li, S.-Z., Li, Q.-S., Huang, D.-D., 2004. Crustal structure of the southern Dabie ultrahigh-pressure orogen and Yangtze foreland from deep seismic reflection profiling. *Terra Nova* 16, 319–324.
- Dong, F., Li, S.-S., Li, Q.-L., Liu, Y.-C., Chen, F.-K., 2007. A preliminary study of common Pb of UHP metamorphic rocks from CCSD (100–2000 m) – evidence for decoupling within subducting continental crust. *Acta Petrologica Sinica* 22, 1791–1798 (in Chinese with English abstract).
- Hacker, B.R., Ratschbacher, L., Webb, L.E., Ireland, T.R., Walker, D., Dong, S., 1998. U/Pb zircon ages constrain the architecture of the ultrahigh-pressure Qinling–Dabie orogen, China. *Earth and Planetary Science Letters* 161, 215–230.
- Hacker, B.R., Ratschbacher, L., Webb, L.E., McWilliams, M.O., Ireland, T., Calvert, A., Dong, S.-W., Wenk, H.-R., Chateigner, D., 2000. Exhumation of ultrahigh-pressure continental crust in east central China: Late Triassic–Early Jurassic tectonic unroofing. *Journal of Geophysical Research* 105, 13339–13364.
- Huang, F., Li, S.-G., Dong, F., Li, Q.-L., Chen, F.-K., Wang, Y., Yang, W., 2007. Recycling of deeply subducted continental crust in the Dabie Mountains, central China. *Lithos* 96, 151–169.
- Huang, F., Li, S.-G., Dong, F., He, Y.-S., Chen, F.-K., 2008. High-Mg adakitic rocks in the Dabie orogen, central China: implications for foundering mechanism of lower continental crust. *Chemical Geology* 255, 1–13.
- Klemme, S., Blundy, J.D., Wood, B.J., 2002. Experimental constraints on major and trace element partitioning during partial melting of eclogite. *Geochimica et Cosmochimica Acta* 66, 3109–3123.
- Kogiso, T., Tatsumi, Y., Nakano, S., 1997. Trace element transport during dehydration processes in the subducted oceanic crust: 1, Experiments and implications for the origin of ocean island basalts. *Earth Planet. Sci. Letter* 148, 193–205.
- Li, S.-G., Xiao, Y., Liu, D., 1993. Collision of the North China and Yangtze blocks and formation of coesite-bearing eclogites: timing and processes. *Chemical Geology*, 109, 89–111.
- Li, S.-G., Wang, S.-S., Chen, Y.-Z., Liu, D.-L., Qiu, J., Zhou, H.-X., Zhang, Z.-M., 1994. Excess argon in phengite from eclogite: evidence from dating of eclogite minerals by Sm–Nd, Rb–Sr and $^{40}\text{Ar}/^{39}\text{Ar}$ methods. *Chemical Geology* 112, 343–350.
- Li, S.-G., Jagoutz, E., Chen, Y., Li, Q., 2000. Sm–Nd and Rb–Sr isotope chronology of ultrahigh-pressure metamorphic rocks and their country rocks at Shuanghe in the Dabie Mountains, central China. *Geochimica et Cosmochimica Acta*, 64, 1077–1093.
- Li, S.-G., Huang, F., Zhou, H.-Y., Li, H.-M., 2003a. U–Pb isotopic compositions of the ultrahigh pressure metamorphic (UHPM) rocks from Shuanghe and gneisses from Northern Dabie zone in the Dabie Mountains, central China: constraint on the exhumation mechanism of UHPM rocks. *Science in China (Series D)* 46, 200–209.
- Li, Q.-L., Li, S.-G., Zheng, Y.-F., Li, H.-M., Massonne, H.J., Wang, Q.-C., 2003b. A high precision U–Pb age of metamorphic rutile in coesite-bearing eclogite from the Dabie Mountains in central China: a new constraint on cooling history. *Chemical Geology* 200, 255–265.

- Li, Q.-L., Li, S.-G., Hou, Z.-H., Hong, J.-A., Yang, W., 2005a. A combined study of SHRIMP U–Pb dating, trace element and mineral inclusions on high-pressure metamorphic overgrowth zircon in eclogite from Qinglongshan in the Sulu terrane. *Chinese Science Bulletin* 50, 459–465.
- Li, S.-G., Li, Q.-L., Hou, Z.-H., Yang, W., Wang, Y., 2005b. Cooling history and exhumation mechanism of the ultrahigh-pressure metamorphic rocks in the Dabie Mountains, central China. *Acta Petrologica Sinica* 21, 1117–1124 (in Chinese with English abstract).
- Liu, F.-L., Xu, Z.-Q., Katayama, I., Yang, J.-S., Maruyama, S., Liou, J.-G., 2001. Mineral inclusions in zircons of pre-pilot drillhole CCSD-PP1, Chinese Continental Scientific Drilling Project. *Lithos* 59, 199–215.
- Liu, F.-L., Xu, Z.-Q., Xue, H.-M., 2004. Tracing the protolith, UHP metamorphism, and exhumation ages of orthogneisses from the SW Sulu terrane (eastern China): SHRIMP U–Pb dating of mineral inclusion-bearing zircons. *Lithos* 78, 411–429.
- Liu, Y.-C., Li, S., Xu, S., Jahn, B.-M., Zheng, Y.F., Zhang, Z., Jiang, L., Chen, G., Wu, W., 2005a. Geochemistry and geochronology of eclogites from the northern Dabie Mountains, central China. *Journal of Asian Earth Sciences* 25, 431–443.
- Liu, F.-L., Liou, J.G., Xu, Z.-Q., 2005b. U–Pb SHRIMP ages recorded in the coesite-bearing zircon domains of paragneisses in the southwestern Sulu terrane, eastern China: new interpretation. *American Mineralogist* 90, 790–800.
- Liu, Y.-C., Li, S.-G., Xu, S.-T., 2007. Zircon SHRIMP U–Pb dating for gneisses in northern Dabie high T/P metamorphic zone, central China: implications for decoupling within subducted continental crust. *Lithos* 96, 170–185.
- Massonne, H.J., 2005. Involvement of crustal material in delamination of the lithosphere after continent–continent collision. *International Geology Review* 47, 792–804.
- Meissner, R., Mooney, W., 1998. Weakness of the lower continental crust: a condition for delamination, uplift, and escape. *Tectonophysics* 296, 47–60.
- Rowley, D.B., Xue, F., Tucker, R.D., Peng, Z.X., Baker, J., Davis, A., 1997. Ages of ultrahigh pressure metamorphism and protolith orthogneisses from the eastern Dabie Shan: U/Pb zircon geochronology. *Earth and Planetary Science Letters* 151, 191–203.
- Rumble, D., Yui, T.-F., 1998. The Qinglongshan oxygen and hydrogen isotope anomaly near Donghai in Jiangsu Province, China. *Geochimica et Cosmochimica Acta* 62 (20), 3307–3321.
- Taylor Jr., H.P., 1990. Oxygen and hydrogen isotope constraints on the deep circulation of surface water into zones of hydrothermal metamorphism and melting. In: Norton, D.L., Bredehoeft, J.D. (Eds.), *The Role of Fluids in Crustal Processes: Studies in Geophysics*. National Academy Press, Washington DC, pp. 72–95.
- Wang, Y.-J., Fan, W.-M., Peng, T.-P., Zhang, H.-F., Duo, F., 2005. Nature of the Mesozoic lithospheric mantle and tectonic decoupling beneath the Dabie Orogen, Central China: evidence from $^{40}\text{Ar}/^{39}\text{Ar}$ geochronology, elemental and Sr–Nd–Pb isotopic compositions of early Cretaceous mafic igneous rocks. *Chemical Geology* 220, 165–189.
- Xiao, Y.-L., Hoefs, J., van den Kerkhof, A.M., Li, S.-G., 2001. Geochemical constraints of the eclogite and granulite facies metamorphism as recognized in the Raobazhai complex from North Dabie Shan, China. *Journal of Metamorphic Geology* 19, 3–19.
- Xiao, Y.-L., Hoefs, J., van den Kerkhof, A.M., Simon, K., Fiebig, J., Zheng, Y.-F., 2002. Fluid history during HP and UHP metamorphism in Dabie Shan, China: constraints from mineral chemistry, fluid inclusions, and stable isotopes. *Journal of Petrology* 43, 1505–1527.
- Xiao, Y.-L., Zhang, Z.-M., Hoefs, J., Kerkhof, A., 2006. Ultrahigh-pressure metamorphic rocks from the Chinese Continental Drilling Project – II Oxygen isotope and fluid inclusion distributions through vertical sections. *Contribution Mineral Petrology* 152, 443–458.
- Xu, S.-T., Okay, A.I., Ji, S., Sengör, A.M.C., Su, W., Liu, Y.-C., Jiang, L.-L., 1992. Diamond from the Dabie Shan metamorphic rocks and its implication for tectonic setting. *Science* 256, 80–82.
- Xu, Z.-Q., Zhang, Z.-M., Liu, F.-L., Yang, J.-S., Tang, Z.-M., Chen, S.-Z., Cai, Y.-C., Li, T.-F., Chen, F.-Y., 2004. The structure profile of 0–1000 m in the main borehole, Chinese Continental Scientific Drilling and its preliminary deformation analysis. *Acta Petrologica Sinica* 20 (1), 53–72 (in Chinese with English abstract).
- Xu, Z.-Q., Zeng, L.-S., Liu, F.-L., Yang, J.-S., Zhang, Z.-M., Williams, M.Mc., Liou, J.G., 2006a. Polyphase subduction and exhumation of the Sulu high-pressure–ultrahigh-pressure metamorphic terrane. *Geological Society of America Special Paper* 403, 93–113.
- Xu, Z.-Q., Wang, Q., Chen, F.-Y., Liang, F.-H., Tang, Z.-M., 2006b. Fabric kinematics of eclogite and deep continental subduction: EBSD study of eclogite from the main hole of the Chinese Continental Scientific Drilling Project. *Acta Petrologica Sinica* 22 (7), 1799–1809.
- You, Z.-D., Su, S.-G., Liang, F.-H., Zhang, Z.-M., 2004. Petrography and metamorphic deformation history of the ultrahigh-pressure metamorphic rocks from the 100–2000 m core of Chinese Continental Scientific Drilling, China. *Acta Petrologica Sinica* 20 (1), 43–52 (in Chinese with English abstract).
- Yui, T.-F., Rumble, D., Luo, C.-H., 1995. Unusually low $\delta^{18}\text{O}$ ultra-high-pressure metamorphic rocks from Sulu Terrain, eastern China. *Geochimica et Cosmochimica Acta* 59 (13), 2859–2864.
- Zartman, R.E., Doe, B.R., 1981. Plumbotectonic – the model. *Tectonophysics* 75, 135–162.
- Zhang, L.-G., 1995. Block-Geology of Eastern Asia Lithosphere – Isotope Geochemistry and Dynamics of Upper Mantle, Basement and Granite. Science Press, Beijing. (in Chinese with English abstract).
- Zhang, R.Y., Hirajima, T., Banno, S., et al., 1995. Petrology of ultra-high-pressure rocks from the southern Su–Lu region, eastern China. *Journal of Metamorphic Geology* 13, 659–675.
- Zhang, H.-F., Gao, S., Zhang, B.-R., et al., 2001. Pb isotope study on crustal structure of Dabie mountains, central China. *Geochimica* 30, 395–401 (in Chinese with English abstract).
- Zhang, Z.-M., Xu, Z.-Q., Liu, F.-L., You, Z.-D., Shen, Q., Yang, J.-S., Li, T.-F., Chen, S.-Z., 2004. Petrological geochemistry of eclogites from the drilling core (100–2050 m) at main hole of the Chinese Continental Scientific Drilling (CCSD) project. *Acta Petrologica Sinica* 20 (1), 27–42 (in Chinese with English abstract).
- Zhang, Z.-M., Xiao, Y.-L., Zhao, X.-D., Shi, C., 2006. Fluid-rock interaction during the continental deep subduction: oxygen isotopic profile of the main hole of the CCSD project. *Acta Petrologica Sinica* 22 (7), 1941–1951.
- Zhao, Z.-F., Zheng, Y.-F., Chen, B., Wu, Y.-B., 2005. A geochemical study of element and Sr–Nd isotopes for eclogite and gneiss from CCSD core 734 to 933 m. *Acta Petrologica Sinica* 21 (2), 325–338 (in Chinese with English abstract).
- Zheng, Y.-F., Fu, B., Gong, B., Li, S.-G., 1996. Extreme ^{18}O depletion in eclogite from the Su–Lu terrane in East China. *European Journal of Mineralogy* 8, 317–323.
- Zheng, Y.-F., Fu, B., Gong, B., Li, L., 2003. Stable isotope geochemistry of ultrahigh pressure metamorphic rocks from the Dabie–Sulu orogen in China: implications for geodynamics and fluid regime. *Earth-Science Reviews* 62, 105–161.
- Zindler, A., Hart, S., 1986. Chemical geodynamics. *Annual Reviews Earth Planet Science* 14, 493–571.